Available online at www.sciencedirect.com
SCIENCE DIRECT®
Journal of Magnetic Resonance 172 (2005) 191–200
JMR Journal of Magnetic Resonance
www.elsevier.com/locate/jmr

Backbone-only restraints for fast determination of the protein fold: The role of paramagnetism-based restraints. Cytochrome b_{562} as an example

Lucia Banci, Ivano Bertini*, Isabella C. Felli, Josephine Sarrou[1]

CERM and Department of Chemistry, University of Florence, Sesto Fiorentino, Italy

Received 27 January 2004; revised 8 July 2004
Available online 2 December 2004

Abstract

CH^{α} residual dipolar couplings (Δrdc's) were measured for the oxidized cytochrome b_{562} from *Escherichia coli* as a result of its partial self-orientation in high magnetic fields due to the anisotropy of the overall magnetic susceptibility tensor. Both the low spin iron (III) heme and the four-helix bundle fold contribute to the magnetic anisotropy tensor. CH^{α} Δrdc's, which span a larger range than the analogous NH values (already available in the literature) sample large space variations at variance with NH Δrdc's, which are largely isooriented within α helices. The whole structure is now significantly refined with the chemical shift index and CH^{α} Δrdc's. The latter are particularly useful also in defining the molecular magnetic anisotropy parameters. It is shown here that the backbone folding can be conveniently and accurately determined using backbone restraints only, which include NOEs, hydrogen bonds, residual dipolar couplings, pseudocontact shifts, and chemical shift index. All these restraints are easily and quickly determined from the backbone assignment. The calculated backbone structure is comparable to that obtained by using also side chain restraint. Furthermore, the structure obtained with backbone only restraints is, in its whole, very similar to that obtained with the complete set of restraints. The paramagnetism based restraints are shown to be absolutely relevant, especially for Δrdc's.

Keywords: Residual dipolar couplings; NMR; b_{562}; Paramagnetic; Solution structure determination

1. Introduction

Residual dipolar couplings (Δrdc's) represent a great advancement in the NMR methodology for solution structure determination [1,2]. They arise from not complete averaging of dipolar interactions in solution and carry a great deal of structural information. Despite this effect was known since the early days of NMR [3], only a few years ago NMR experiments were introduced to actively exploit Δrdc's for solution structure determination [4–7]. Several approaches to increase the partial alignment of macromolecules in solution have been proposed including liquid crystals [4,8,9], purple membrane fragments [10], filamentous phages [11], mineral liquid crystals [12], and other media [13–15]. A most straightforward approach, however, is that of exploiting the natural magnetic anisotropy of molecules which induces spontaneous orientation in high magnetic fields. This approach does not require the use of external media and thus is the least perturbative. In this respect paramagnetic metal centers, characterized by anisotropic magnetic susceptibilities, provide significant additional contributions to the overall anisotropy of the magnetic susceptibility [1,16–20]. It was soon shown that Δrdc's, as measured, are consistent with pseudocontact shifts

* Corresponding author. Fax: +39 055 4574271.
E-mail address: bertini@cerm.unifi.it (I. Bertini).
[1] Present address: Department of Chemistry, University of California, Davis, CA, USA.

1090-7807/$ - see front matter © 2004 Elsevier Inc. All rights reserved.
doi:10.1016/j.jmr.2004.07.024

and NOEs [5]. In the very same research [5], the structures were calculated through the completely anisotropic magnetic susceptibility tensor while at the same time a simulation calculation was reported [21].

In principle, the dipolar interaction between any pair of nuclei contains structural information in terms of orientation of the nucleus–nucleus vector in the molecular frame. In practice, specific pairs of nuclei should be identified that give measurable effects. Residual dipolar couplings of NH systems were first proposed [2] and are the most popular in structure determination. Backbone CH^{α} Δrdc's are more seldom used [7]. However, if compared to NH Δrdc's, they are expected to be larger, due to the larger γ of the ^{13}C nucleus, and to span a larger range of values. This implies that CH^{α} Δrdc's can be more accurately measured also from self-orientation in high magnetic fields even if the molecular magnetic susceptibility is relatively modest. Furthermore, CH^{α} vectors sample a larger range of orientations with respect to NH vectors, especially in secondary structural elements such as α helices and, to a minor extent, in β sheets.

CH^{α} and NH Δrdc's are some of the observables which can be easily available in the first stages of assignment and structure calculations. For this reason, they are very appealing as restraints to speed up the process of backbone folding. Several attempts to use residual dipolar couplings, mainly measured in heavily orienting media, as a shortcut to structure determination in solution or to validate structural models have been proposed [8,22–29]. Other kinds of backbone restraints (hydrogen bonds, CSI, and NOEs) were also shown very useful to quickly determine a structural model [29–31].

We wanted here to evaluate the impact of paramagnetism based backbone restraints, in particular of backbone pseudocontact shifts and of residual dipolar couplings (CH^{α} and NH Δrdc's), on quick fold structure determination, when used in combination with other "diamagnetic" backbone restraints such as hydrogen bonds, CSI, NOEs, and ^{3}J couplings. We chose for this purpose the oxidized cytochrome b_{562} which has already been well characterized. Oxidized cytochrome b_{562} contains a low spin iron (III) heme whose relatively small magnetic anisotropy is responsible for partial self orientation [32,33]. Also the four helix bundle fold contributes to the overall magnetic anisotropy [34]. The solution structure of this protein is available, determined with all the restrains but CSI and CH^{α} Δrdc's [33,34]. Here, we measure CH^{α} Δrdc's and then we evaluate the contribution of the above mentioned different classes of backbone restraints on the "quick" determination of the protein fold. This research shows the relevance of the paramagnetism based restraints. Furthermore, we also show the impact of these CH^{α} Δrdc's additional restraints on the complete structure determination and on the determination of the magnetic susceptibility tensor.

2. Results and discussion

2.1. NMR experiments

Assignment of ^{13}C resonances of oxidized cytochrome b_{562} was not available. For this purpose, two 3D experiments (CBCACONH and CBCANH) were analyzed to extend the backbone assignment to C^{α} and C^{β}. 2D HCCH COSY experiments were then analyzed to correlate the ^{13}C assignment to the ^{1}H. Carbon assignment (C^{α} and C^{β}) was achieved to 96% of the residues. It is reported in Table 1 of the supplementary material.

The experiment used to measure CH^{α} Δrdc's was a *J*-modulated experiment [35] very similar to the one used to determine NH Δrdc's [2]. The main difference between the two experiments is a constant time evolution in the indirect ^{13}C dimension to refocus C–C couplings in the case of CH^{α} groups. The experiments were repeated at two different magnetic fields (18.8 and 9.4 T). Great care was taken to optimize the selectivity of pulses on the carbon channel because small deviations can prevent observation of signals. In the ^{1}H–^{13}C *J*-modulated experiments, 52 cross peaks of CH^{α} groups were sufficiently well resolved at both magnetic fields to determine Δrdc's (which compares with the 67 NH Δrdc's previously determined [34]).

The measured CH^{α} Δrdc's are reported together with NH Δrdc's in Fig. 1 and in Table 2 of the supplementary material. As expected (see Section 3) the CH^{α} Δrdc's

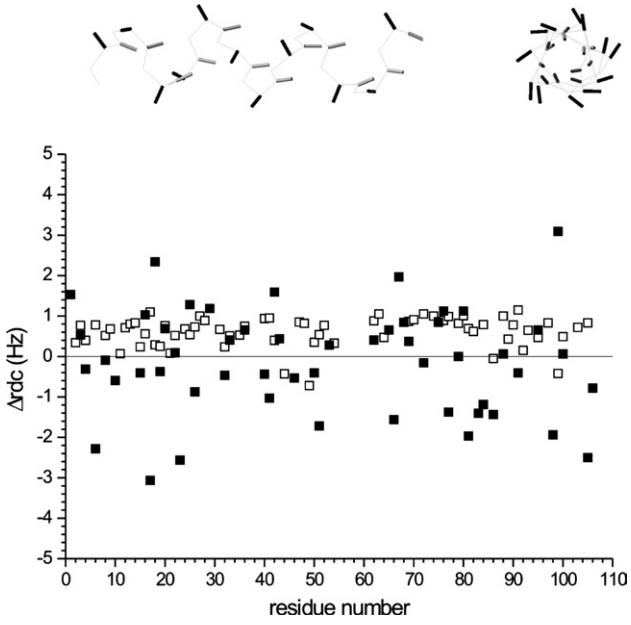

Fig. 1. Residual dipolar couplings determined for oxidized cytochrome b_{562} (filled symbols are CH^{α} Δrdc's and open symbols are NH Δrdc's [34]). The inset shows the orientation of CH^{α} (black) and NH (grey) vectors in a α helix.

span a larger range of values than NH Δ*rdc*'s. Furthermore in the present system, the NH Δ*rdc*'s are essentially all positive. This behavior is due to the peculiar fold of the present protein, which contains four α helices, roughly oriented in the same direction. NH vectors, whose direction is nearly aligned with the helix axis, have very similar values within a helix, while CH^{α} vectors sample different orientations. This property clearly points out the relevance of the CH^{α} vector orientation in structural calculations.

Another structural parameter can be easily obtained from the $^{13}C^{\alpha}$ chemical shift index (CSI), which is determined by comparing the experimental $^{13}C^{\alpha}$ chemical shifts with the average chemical shifts database [36]. The CSI is strongly related to the presence of secondary structure elements. In oxidized cytochrome b_{562}, CSI allowed us to predict α helices in the following regions: 3–18 (α_1), 23–41 (α_2), 59–80 (α_3), and 84–100 (α_4).

2.2. Structure calculations using all restraints

The Δ*rdc*'s and CSI restraints were used, together with all already available constraints, to calculate a more accurate and precise structure. The agreement between experimental and calculated residual dipolar couplings obviously improves after inclusion of residual dipolar couplings in structure calculations (the RMS difference between experimental and calculated Δ*rdc*'s goes from 0.27 to 0.20 Hz, Fig. 2). Furthermore, CH^{α} Δ*rdc*'s contribute to a better sampling of the Δ*rdc*'s range. The resulting family of conformers (Fig. 3) has RMSD to the mean structure of 0.38 Å (with a variability of 0.08 Å) and 0.88 Å (with a variability of 0.07 Å) for backbone and heavy atoms respectively, and a total target function [5,60,62,63] of 1.65 ± 0.12 Å^2. The solution structure previously available is characterized by RMSD to the mean structure of 0.50 Å (with a variability of 0.10 Å) and 1.03 Å (with a variability of 0.11 Å) for backbone and heavy atoms, respectively, and a target function [5,60,62,63] of 1.34 ± 0.12 Å^2 [34]. The RMSD per residue shows an improvement in the resolution of the regions 25–48 and 62–100. This is due in part to an improved local definition of the helices, as can be observed from local RMSD values (data not shown) and in part to more accurate positioning of the helices deriving from long range structural restraints, such as pseudocontact shifts and residual dipolar couplings. Indeed, if pseudocontact shifts, residual dipolar couplings, and CSI derived restraints are not used in structure calculations the RMSD to the mean structure becomes 0.48 Å (with a variability of 0.10 Å) and 0.97 Å (with a variability of 0.10 Å) for backbone and heavy atoms, respectively.

The use of CH^{α} Δ*rdc*'s in structure calculations, in addition to NH Δ*rdc*'s, contributes to the definition of the total magnetic susceptibility tensor. This is particularly true in the case of cytochrome b_{562} because of the peculiar fold of the protein in which NH bond vectors sample a rather limited subset of orientations. Therefore CH^{α} bond vectors contribute to a better sampling of directions in space and thus to a more accurate tensor. The tensor obtained after inclusion of CH^{α} Δ*rdc*'s in structure calculations is in good agreement with the one previously determined using

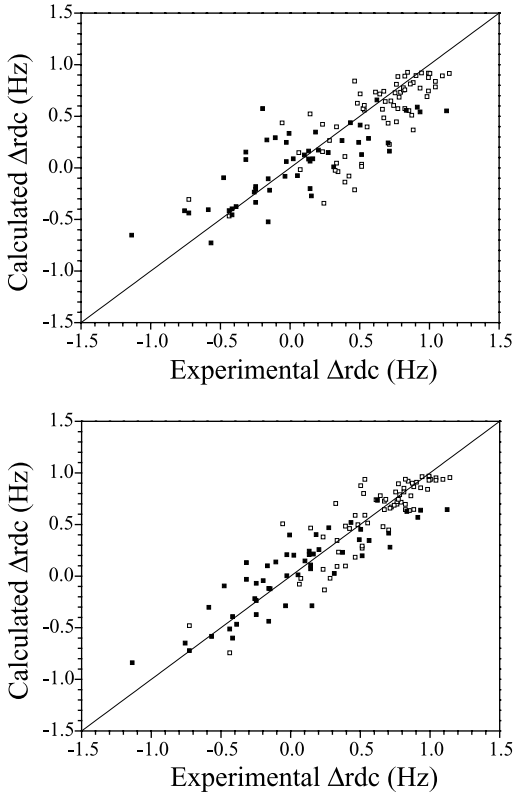

Fig. 2. Calculated versus experimental Δ*rdc* values for CH^{α} (filled squares) and NH (open squares) moieties are reported for the structure calculated without (top) and with (bottom) Δ*rdc*'s. The RMS difference between experimental and calculated Δ*rdc*'s goes from 0.27 (top) to 0.20 Hz (bottom). The values reported for CH^{α} groups are scaled as described in Section 3.

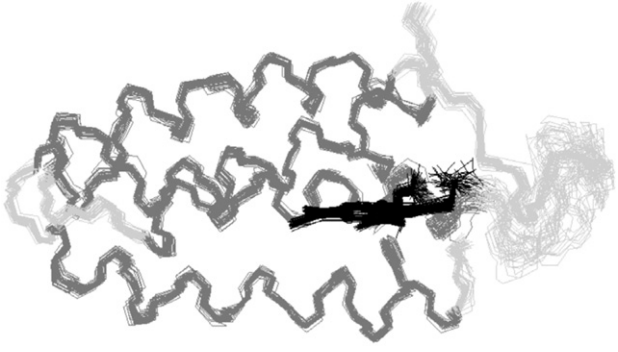

Fig. 3. Structure of oxidized b_{562} calculated using the complete set of available restraints. Only the backbone, the heme and the two iron ligands are shown. The heme is shown in black, helices are shown in dark grey, the remaining parts of the backbone are shown in light grey.

Table 1
Molecular χ tensor parameters of oxidized cytochrome b_{562} estimated using the family of conformers calculated with all available experimental restraints

	NH + CH	From structure defined only with NH Δrdc's [34]
$\Delta\chi_{ax}$ ($/10^{-32}$)	-1.9 ± 0.05	-2.0 ± 0.4
$\Delta\chi_{rh}$ ($/10^{-32}$)	0.7 ± 0.08	0.5 ± 0.3
Deviation of the z axis from from the normal to the heme plane (°)	86 ± 9	98 ± 8
Deviation of the y axis from the heme pyrrole Nβ–Nδ axis (°)	87 ± 10	74 ± 15

For comparison, the values previously obtained employing only NH Δrdc's are also reported.

only NH Δrdc's with a better definition of the anisotropy values (Table 1) [34].

2.3. Folding calculations using only backbone restraints

Analysis of backbone CSI and determination of CH^{α} Δrdc's yields two additional types of experimental structural restraints that can be available right after backbone assignment. These are particularly important for structure determination of proteins characterized by low NOE density, such as large proteins, or when time restraints push to quick structure determination. In the frame of assessing the contribution of each class of experimental restraint for speeding up the process of backbone fold determination, we have performed folding calculations using the various types of restraints that can be determined using only backbone assignment. More specifically the set of restraints that we will consider here are backbone NOEs, $^{3}J_{HNH\alpha}$, hydrogen bonds, pseudocontact shifts, NH and CH^{α} Δrdc's, and CSI. We will refer to this set as "backbone" restraints. The results of calculations carried out with different subsets of "backbone" restraints and compared with the structure calculated using all available restraints (previous paragraph) are reported in Table 2. Several conclusions can be drawn from this table.

The backbone structure obtained with the complete set of backbone restraints is very similar to that of the complete structure. This shows that this set of restraints is sufficient to determine the 3D fold with good accuracy. Let us then analyze in detail the contribution of each type of experimental backbone restraint. NOE restraints, at least with the calculation program employed and with the set of restraints available (see later), are necessary to obtain the correct 3D fold. However, they are not sufficient as the elements of secondary structure present in the protein are barely defined (RMSD above 7 Å), and only a rough indication of their relative orientation is obtained (Fig. 4A). Addition of dihedral angle restraints and hydrogen bond restraints contributes to a better definition of the elements of secondary structure but the correct definition of the helices reciprocal orientation is not determined yet (Fig. 4B and Table 2). The contribution of the CSI derived restraints is instead dramatic and the RMSD drops down to 2.6 Å (Fig. 4C). Therefore, the "diamagnetic" backbone restraints are well suited to define the secondary structural elements and the 3D fold. However, as it can be observed in Fig. 4C, the relative orientation of helices

Table 2
Results of structural calculations using different subsets of backbone-only structural restraints on oxidized cytochrome b_{562}

Used constraints						Structure statistics				
NOE	J	HB	CSI	PCS	RDC	RMSD (Å)				T (Å^2)
						BB[a]	Variability[a]	HA[a]	Variability[a]	
X	x	x	x	x	x	1.74	0.47	2.76	0.47	0.94–2.50
X	x	x	x	x		2.88	2.57	3.86	2.65	0.14–0.47
X	x	x	x			2.61	2.16	3.68	2.25	0.08–0.31
	x	x	x			13.07	3.56	14.10	3.37	0.002–0.03
	x	x	x	x	x	12.70	3.22	13.75	3.03	2.00–3.30
X						7.53	3.35	8.92	3.32	0.40–1.38
X	x	x	x		x	1.90	0.45	2.96	0.47	0.38–1.37
X	x	x	x		NH	1.87	0.38	2.85	0.4	0.15–0.84
X	x	x	x		CH	1.87	0.37	2.94	0.42	0.25–0.94
X	x	x		x	x	2.83	0.57	3.88	0.71	1.13–4.8
X	x	x		x		6.19	3.28	7.45	3.25	0.155–2.9
X	x	x				6.36	3.03	7.65	3.01	0.11–2.73
X	x	x	x	x	CH	3.59	2.88	4.67	2.93	0.4–2.0
X	x	x	x	x	NH	2.34	1.46	3.88	1.53	0.33–1.47

For each calculation, the table indicates the kind of restraint used (NOE, J couplings, hydrogen-bonds, chemical shift index, pseudocontact shifts, and residual dipolar couplings), the RMSD for backbone (RMSD-BB), heavy atoms (RMSD-HA), and the target function (T) [5,60,62,63]. The RMSD values reported are average values over the conformers constituting the family of structures. The statistics refer to families of 40 conformers.

[a] BB and HA indicate the average RSMD values for the backbone and heavy atoms, respectively. Variability represent the range of values of these two quantities.

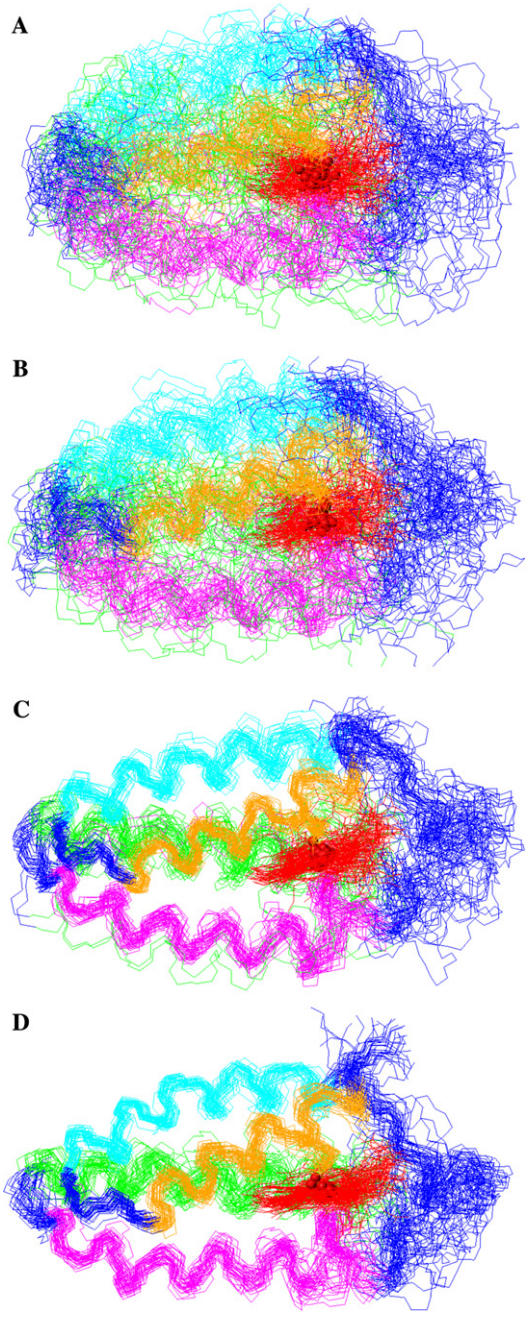

Fig. 4. Structures of oxidized cytochrome b_{562} using different subsets of backbone restraints (see text). The restraints are: backbone NOEs only (A); backbone NOEs, $^3J_{HNH\alpha}$, and hydrogen bond restraints (B); backbone NOEs, $^3J_{HNH\alpha}$, hydrogen bond restraints, and CSI, (C); and backbone NOEs, $^3J_{HNH\alpha}$, hydrogen bond restraints, CSI, NH and CH^{α} Δrdc's (D). Only the backbone, the heme, and the iron ligands are shown. The heme is shown in red, helix α_1 is shown in orange, α_2 in cyan, α_3 in green, and α_4 in magenta, the remaining parts of the backbone are shown in blue.

α3 (green) and α4 (magenta) is not yet unequivocally defined by only the "diamagnetic" backbone restraints. The relative orientation of α helices is readily determined when the "orientational restraints," represented by Δrdc's, are applied. Pseudocontact shifts also contribute, but they alone are not sufficient to determine the relative orientation of the two helices. The combined use of Δrdc's and pseudocontact shifts produces a sizeable improvement of the resolution (Fig. 4D). Backbone RMSD values per residue are reported in Fig. 5. The relative contributions of CH^{α} and NH Δrdc's are very similar. If CH^{α} and NH Δrdc's are included separately in two distinct calculations the obtained structures have the correct 3D fold. The combined use of the two sets of Δrdc's leads to a better resolution of the structure.

Concluding, the accuracy of the structure obtained using "backbone-only" constraints, which can be evaluated comparing it to the structure obtained with all available structural constraints, strongly depends on the different types of structural constraints employed. In other words, each set of constraints appears to have a specific role and at the same time also contributes to obtain a better agreement of the structure with the other sets of restraints. Indeed only the combined use of NOEs, hydrogen bonds, ^3J couplings, CSI constraints with long range orientational constraints such as NH, CH^{α} Δrdc's, and pseudocontact shifts allows us to obtain the structure reported in Fig. 4D (relative structural parameters are reported in Table 2), characterized by a fairly good resolution and by a correct placing of secondary structural elements, i.e., by the correct backbone fold. Cross-validation [64,65] of NH, CH^{α} Δrdc's, and CSI constraints was performed following the standard procedure, as described in Section 3 on both the all restraint structure and on the backbone only restraint structure. The results (Tables 3A and B of the supplementary material) indicate the high accuracy of the structures, as shown by the agreement between the experimental restraints and their values calculated using a structure obtained without their inclusion (as indicated by no significant increase in the total restraint target values). Also the structures obtained with the exclusion of

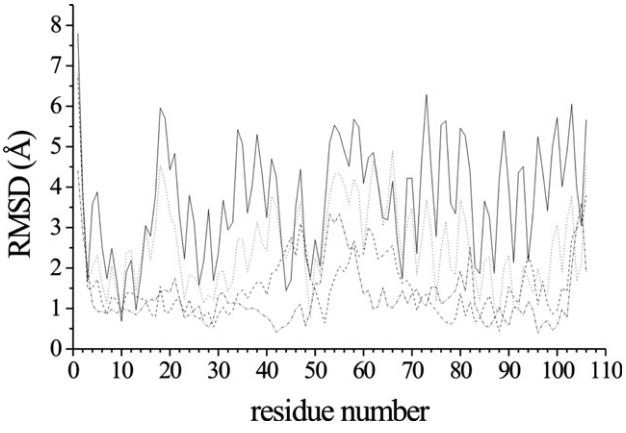

Fig. 5. Average backbone RMSD per residue between the mean structure obtained with all experimental restraints, and the mean structure of the four types of calculations reported in Fig. 3. (A) continous line, (B) dots, (C) dashes, and (D) dashes and dots.

various sets of constraints do not differ from the reference structure.

It is then interesting to check what happens to the side chain conformations when the set of backbone-only restraints is used. The comparison between the family of structures obtained with the "backbone-only" set of restraints and that obtained with all restraints indicates that the former is obviously characterized by a lower resolution but it also indicates that no significantly different conformations for side chains are observed (the heavy atom RMSD between the two average structures is never larger than the sum of the two heavy atom RMSD values within each family, Fig. 1, supplementary material). Moreover, it is interesting to note that for the vast majority of residues in well defined secondary structural elements (77% of the 74 residues analyzed) the χ_1 angle is well reproduced (if compared to the structure obtained with all experimental structural constraints), despite no constraints at all were used for side chains. Out of the remaining residues in well defined secondary structural elements, 11 adopt more than one rotameric state (one of which is the one present in the structure obtained with all experimental restraints) and only six resides exhibit a different conformation.

An initial estimate of the χ tensors is needed for applying paramagnetic and orientation dependent restraints. In the present case such estimates are available from the previously determined structure through the programs fantasian [37,38] and fantaOrient [5]. In general, however the initial estimates are unknown. For this reason we verified that the overall magnetic susceptibility tensor could be determined from scratch relying only on backbone restraints. We initially estimated the tensor parameters from the structures obtained with "diamagnetic" backbone restraints only. After a few cycles of these calculations, the structure and tensor parameters converge, with a deviation lower than 5% in each step. The tensor parameters agree, within 10%, with those determined on the structure obtained using all experimental constraints. It is interesting to note that the initial estimates of the overall magnetic susceptibility tensor, which determines the molecular alignment, using as input CH^{α} and NH Δrdc's and a structure obtained without them, are very similar to the final values. Instead, this tensor is difficult to define when only NH Δrdc's are used, making CH^{α} Δrdc's important for structure calculations using backbone restraints.

2.4. Concluding remarks

Several approaches have been recently proposed to speed up the process of structure determination [22,23,30,31,39,40]. This is a fast developing field especially in the light of structural genomics projects. Residual dipolar couplings, due to the ease of their determination and to their high information content have been actively exploited. It has been shown [23] that, provided a large number of Δrdc's per residue are available, the complete 3D fold can be determined without any other type of structural restraints. A convenient approach that does not require external alignment media relies on magnetic field induced alignment of paramagnetic metalloproteins characterized by large magnetic anisotropy. This approach has been explored with lanthanide metal ions, either substituting Ca^{2+} in calcium binding proteins [16,41–43] or using a lanthanide binding tag [44,45]. In many biologically relevant cases, there is one or more low spin iron (III) hemes which induces a modest but measurable alignment [5,34]. In the present study, we restricted ourselves to Δrdc's involving at least one proton. Indeed, the residual dipolar couplings involving two directly bound heteronuclei (C–C or C–N) are usually much smaller than the ones involving at least one proton due to the lower gyromagnetic ratios and to the larger internuclear distance between the two heteronuclei (for example, if compared to NH Δrdc's, C–N are expected to be 10 times smaller, C–C about 5–6 times smaller). These are thus very difficult to measure in case of modest alignment. On the other hand, anisotropic paramagnetic metal ions have the advantage of further providing a wealth of easily accessible structural information [40] including pseudocontact shifts [20,37,38,41,46], relaxation rate enhancements [47–49], and cross correlation rates [20,50,51].

In the present study, besides refining a previously determined structure, we have explored the possibility of determining the protein fold by using backbone restraints. The latter are easily available after backbone assignment. The results indicate that this set of backbone restraints (backbone NOEs, ^{13}C CSI, H-bonds, pseudocontact shifts, and NH and CH^{α} Δrdc's) is sufficient to accurately determine the correct 3D fold of the protein. In this respect, particularly useful are the CSI restraints, which define the elements of secondary structure and the NH and CH^{α} Δrdc's, which define their relative orientation. Pseudocontact shifts and possibly long range backbone NOEs refine the backbone structure.

3. Experimental

3.1. Sample preparation

^{15}N-, ^{13}C-labeled cytochrome b_{562} from *Escherichia coli* was prepared as previously described [33,52]. The samples used for NMR spectroscopy, either in D_2O or in 90% H_2O and 10% D_2O, were about 2.5 mM in 500 mM phosphate buffer at pH 5.0. Cytochrome b_{562} is present in solution in two forms that differ by a 180° rotation of the heme plane. We will hereafter consider the major isomer.

3.2. NMR spectroscopy

NMR experiments were acquired with Bruker instruments of the Avance series operating at 9.4 T (400 MHz), 16.4 T (700 MHz), and 18.8 T (800 MHz) at 298 K. All NMR spectrometers were equipped with ^{1}H, ^{13}C, and ^{15}N TXI probes with z pulsed field gradients except the 400 MHz instrument, where the probe BBO was used. All NMR experiments were acquired at 300 K.

The experiments acquired to assign Cα and Cβ spins were: 3D CBCACONH [53], 3D CBCANH [54], and a few 2D COSY-HCCH [55] experiments. ^{13}C chemical shifts were referenced to the dioxane signal (aqueous, 10%, 298 K) at 69.46 ppm [36]. These were acquired in H_2O at 700 MHz with the standard parameters.

Experiments to determine $^{1}J_{CH}$ were acquired in D_2O at 400 MHz and at 800 MHz. The sequence used was the one proposed by Tjandra and Bax [35]. Quadrature detection in the indirect dimension was obtained through TPPI of the first ^{13}C 90° pulse. The relaxation delay was 1 s. The increment in the indirect dimension was 25 μs. The sweep width in the ^{1}H dimension was 8000 Hz and 2048×512 data points were acquired in the ^{1}H and ^{13}C dimensions, respectively. The ^{13}C carrier was set at 55 ppm. The length of 90° ^{13}C square pulses at 400 MHz and at 800 MHz was 35 and 15 μs, respectively. Selective carbonyl ^{13}C 180° pulses were given with an offset of 125 ppm and Q3 shape [56] with a length of 500 μs and 256 μs at 400 and 800 MHz, respectively. Composite pulse decoupling was applied during acquisition (127 ms) with an RF field strength of 2.5 kHz. The ^{13}C constant time ($2T$) was set to 28 ms. At each magnetic field, the experiment was repeated 17 times changing the time during which the $^{1}J_{CH}$ evolves $2(T - \Delta)$. The delay Δ was thus changed in the range 1.0–6.7 ms. More specifically the values of Δ used were 1.0, 2.2, 2.5, 2.8, 3.1, 3.4, 3.7, 4.0, 4.3, 4.6, 4.9, 5.2, 5.5, 5.8, 6.1, 6.4, and 6.7 ms at 400 MHz and 1.0, 1.3, 1.6, 1.9, 2.2, 2.5, 2.8, 3.1, 3.4, 3.7, 4.0, 4.3, 4.6, 4.9, 5.2, 5.5, and 5.8 ms at 800 MHz. The total experimental time for each series of experiments is about 36 h. Experimental data were processed with Xwinnmr using only 1024×512 points of acquired data to final data matrices of 2048×512 data points using shifted squared cosine functions to enhance resolution. Assignment was performed using the program Xeasy [57].

3.3. Data analysis

The J_{CH} couplings were determined by fitting the intensity of each cross peak versus the delay Δ with a two parameter function:

$$I(T) = A\cos[2\pi J_{CH}(T - \Delta)], \tag{1}$$

where A and J_{CH} are the variable parameters, T is the constant time used in the experiments ($T = 14$ ms) and Δ is the delay changed in the different experiments. The use of only two parameters is a consequence of the constant time evolution in the ^{13}C dimension. The error on the fitting of J_{CH} values was in the range ±0.1 Hz similar to that obtained in analogous experimental conditions [35].

Experimental residual dipolar couplings Δrdc's were determined taking the difference between the values of J_{CH}measured at the two magnetic fields:

$$\Delta rdc(\theta,\phi) = [(J_{800\,\mathrm{MHz}} - J_{400\,\mathrm{MHz}})] + (\delta_{\mathrm{DF800\,MHz}} - \delta_{\mathrm{DF400\,MHz}}). \tag{2}$$

The difference in J_{CH} (see Eq. (2)) in principle also contains the field dependent part of the dynamic frequency shift (δ_{DFS}) [2,58]. The δ_{DFS} for the CH^{α} groups can be estimated adapting the equation already available for NH systems [2,58] to CH^{α} groups. By taking into account in that equation the CSA for carbon [59], which is smaller than for amide nitrogens, the different gyromagnetic ratio, and the different frequencies sampled, the dynamic frequency shift contribution is calculated as negligible and can be safely neglected because it results smaller than the error on the J_{CH} values.

Δrdc's are related to the magnetic anisotropy tensor and to the orientation of the CH^{α} vectors by the following equation:

$$\Delta rdc(\theta,\phi,B_0) = -\frac{1}{4\pi}\frac{B_{\mathrm{high}}^2 - B_{\mathrm{low}}^2}{15kT}\frac{\gamma_H\gamma_X h}{4\pi^2 r_{\mathrm{HX}}^3} \times \left[\Delta\chi_{\mathrm{ax}}(3\cos^2\theta - 1) + \frac{3}{2}\Delta\chi_{\mathrm{rh}}(\sin^2\theta\cos 2\phi)\right], \tag{3}$$

where $\Delta\chi_{ax}$ and $\Delta\chi_{rh}$ are the axial and rhombic anisotropies of the molecular magnetic susceptibility tensor (χ^{mol}), and θ, and ϕ are the polar coordinates describing the orientation of the X–H bond vector in the tensor axis system.

As the NH Δrdc's, previously measured [34], and the CH^{α} Δrdc's here determined were used simultaneously in structure calculations, the difference of the magnetic fields at which the J couplings were measured need to be taken into account. Considering that the low field used for CH^{α} Δrdc's is 400 MHz instead of 500 MHz as for NH Δrdc's, the CH^{α} Δrdc's should span a range that is 2.65 times that of NH Δrdc's, as experimentally observed:

$$\frac{\gamma_c r_{\mathrm{NH}}^3}{\gamma_N r_{\mathrm{CH}}^3}\frac{800^2 - 400^2}{800^2 - 500^2} = -2.65.$$

The program CSI [36] was used to determine restraints on backbone dihedral angles from the chemical shift index (CSI). The information derived from CSI was converted into structural restraints using limits derived from the Ramachandran plot. These were $-130° < \phi < -30°$ and $-60° < \psi < 30°$ for α helices.

Tensor parameters were fitted to the experimental values with the program fantaOrient [5].

3.4. Structure calculations

The program PARAMAGNETICDYANA, an expanded version of the program DYANA [62], was used to perform structure calculations as it allows to include all types of structural restraints available, including also pseudocontact shifts [60] and residual dipolar couplings [5]. In each structure calculation, 400 randomly generated structures were annealed to obtain a family of 40 structures. The relative weight of restraints was one and the tolerance value for Δrdc's was 0.3 Hz. Tensor parameters were estimated using fantasian [37,38] and fantaOrient [5]. These were initially estimated from each member of the family of conformers calculated without them and then were used as input in subsequent calculations until convergence. This procedure was repeated until the tensor parameters did not change more than 5%. Calculations were repeated with all restraints available for backbone nuclei. These include 633 NOE-derived upper distance limits, 18 hydrogen bonds, 32 dihedral angle restraints derived from ^{3}J coupling constants, 126 dihedral angle restraints derived from CSI, 119 residual dipolar couplings and 175 pseudocontact shifts. Also for these calculations the tensor parameters were initially estimated with the previously determined structures and then finalized through iterative structural calculations with this reduced set of constraints, following the same procedure used for the calculations with the complete set of constraints. The RMSD values reported in the text for the calculations using all constraints are calculated to the mean structure of the family considering residues 3–50 and 62–105. For the calculations using "backbone constraints" only instead, the RMSD values are the average values within the family of conformers as, in some of the calculations in this series (Table 2), the average structure may have no meaning (too different conformations are sampled). Cross-validation [64,65] of NH, CH^{α} Δrdc's and CSI constraints was performed considering the complete set of constraints and the "backbone-only" set of constraints; structure calculations were repeated excluding 10% of each set of constraints considered (NH, CH^{α} Δrdc's, and CSI) and this procedure was repeated three times (Table 3, supplementary material). Calculations were performed with a cluster of Linux PCs. The figures were generated with the program MOLMOL [61].

Acknowledgments

This work has been partly supported by SPINE "Structural proteomics in Europe," Contract No. QLG2-CT-2002-00988. J.S. has been supported by the Research Training Network "CROSSCORRELATION," Contract No. HPRN-CT-2000-00092.

Appendix A. Supplementary data

Supplementary data associated with this article can be found, in the online version, at doi:10.1016/j.jmr.2004.07.024.

References

[1] J.R. Tolman, J.M. Flanagan, M.A. Kennedy, J.H. Prestegard, Nuclear magnetic dipole interactions in field-oriented proteins: information for structure determination in solution, Proc. Natl. Acad. Sci. USA 92 (1995) 9279–9283.
[2] N. Tjandra, S. Grzesiek, A. Bax, Magnetic field dependence of nitrogen-proton J splittings in ^{15}N-enriched human ubiquitin resulting from relaxation interference and residual dipolar coupling, J. Am. Chem. Soc. 118 (1996) 6264–6272.
[3] A.A. Bothner-By, Magnetic field induced alignment of molecules, in: D.M. Grant, R.K. Harris (Eds.), Encyclopedia of Nuclear Magnetic Resonance, Wiley, Chichester, 1996.
[4] N. Tjandra, A. Bax, Direct measurement of distances and angles in biomolecules by NMR in a diluite liquid crystalline medium, Science 278 (1997) 1111–1114.
[5] L. Banci, I. Bertini, J.G. Huber, C. Luchinat, A. Rosato, Partial orientation of oxidized and reduced cytochrome b_5 at high magnetic fields: magnetic susceptibility anisotropy contributions and consequences for protein solution structure determination, J. Am. Chem. Soc. 120 (1998) 12903–12909.
[6] I. Bertini, M.B.L. Janik, G. Liu, C. Luchinat, A. Rosato, Solution structure calculations through self-orientation in a magnetic field of cerium (III) substituted calcium-binding protein, J. Magn. Reson. 148 (2001) 23–30.
[7] N. Tjandra, J.G. Omichinski, A.M. Gronenborn, G.M. Clore, A. Bax, Use of dipolar ^{1}H–^{15}N and ^{1}H–^{13}C couplings in the structure determination of magnetically oriented macromolecules in solution, Nat. Struct. Biol. 4 (1997) 732–738.
[8] G. Cornilescu, A. Bax, Measurement of proton, nitrogen, and carbonyl chemical shielding anisotropies in a protein dissolved in a dilute liquid crystalline phase, J. Am. Chem. Soc. 122 (2000) 10143–10154.
[9] I. Bertini, F. Castellani, C. Luchinat, G. Martini, G. Parigi, S. Ristori, Partial orientation of cytochrome-c in a lyotropic liquid crystal: residual H–H dipolar coupling, J. Phys. Chem. 104 (2000) 10653–10658.
[10] B.W. Koenig, H. Jin-Shan, M. Ottiger, S. Bose, R.W. Hendler, A. Bax, NMR measurement of dipolar couplings in proteins aligned by transient binding to purple membrane fragments, J. Am. Chem. Soc. 121 (1999) 1385–1386.
[11] M.R. Hansen, L. Mueller, A. Pardi, Tunable alignment of macromolecules by filamentous phage yields dipolar coupling interactions, Nat. Struct. Biol. 5 (1998) 1065–1074.
[12] H. Desvaux, J.C.P. Gabriel, P. Berthault, F. Camerel, First use of a mineral liquid crystal for measurement of residual dipolar couplings of a nonlabeled biomolecule, Angew. Chem. 40 (2001) 373–376.
[13] G.M. Clore, M.R. Starich, A.M. Gronenborn, Measurement of residual dipolar couplings of macromolecules aligned in the nematic phase of a colloidal suspension of rod-shaped viruses, J. Am. Chem. Soc. 120 (1998) 10571–10572.
[14] L.G. Barrientos, J.M. Louis, A.M. Gronenborn, Characterization of the cholesteric phase of filamentous bacteriophage fd

for molecular alignment, J. Magn. Reson. 149 (2001) 154–158.
[15] L.G. Barrientos, C. Dolan, A.M. Gronenborn, Characterization of surfactant liquid crystal phases suitable for molecular alignment and measurement of dipolar couplings, J. Biomol. NMR 16 (2000) 329–337.
[16] I. Bertini, M.B.L. Janik, Y.-M. Lee, C. Luchinat, A. Rosato, Magnetic susceptibility tensor anisotropies for a lanthanide ion series in a fixed protein matrix, J. Am. Chem. Soc. 123 (2001) 4181–4188.
[17] I. Bertini, I.C. Felli, C. Luchinat, Lanthanide induced residual dipolar couplings for the conformational investigation of peripheral $^{15}NH_2$ moieties, J. Biomol. NMR 18 (2000) 347–355.
[18] I. Bertini, C. Luchinat, NMR of paramagnetic substances, Coord. Chem. Rev. 150 (1996).
[19] M.A. Contreras, J. Ubach, O. Millet, J. Rizo, M. Pons, Measurement of one bond dipolar couplings through lanthanide-induced orientation of a calcium-binding protein, J. Am. Chem. Soc. 121 (1999) 8947–8948.
[20] J.C. Hus, D. Marion, M. Blackledge, De novo determination of protein structure by NMR using orientational and long-range order restraints, J. Mol. Biol. 298 (2000) 927–936.
[21] G.M. Clore, A.M. Gronenborn, N. Tjandra, Direct structure refinement against residual dipolar couplings in the presence of rhombicity of unknown magnitude, J. Magn. Reson. 131 (1998) 159–162.
[22] J. Meiler, W. Peti, C. Griesinger, DipoCoup: a versatile program for 3D-structure homology comparison based on residual dipolar couplings and pseudocontact shifts, J. Biomol. NMR 17 (2000) 283–294.
[23] J.C. Hus, D. Marion, M. Blackledge, Determination of protein backbone structure using only residual dipolar couplings, J. Am. Chem. Soc. 123 (2001) 1541–1542.
[24] J.J. Chou, S. Li, A. Bax, Study of conformational rearrangement and refinement of structural homology models by the use of heteronuclear dipolar couplings, J. Biomol. NMR 18 (2000) 217–227.
[25] A. Annila, H. Aitio, E. Thulin, T. Drakenberg, Recognition of protein folds via dipolar couplings, J. Biomol. NMR 14 (1999) 223–230.
[26] F. Delaglio, G. Kontaxis, A. Bax, Protein structure determination using molecular fragment replacement and NMR dipolar couplings, J. Am. Chem. Soc. 122 (2000) 2142–2143.
[27] B.A. Fowler, F. Tian, H.M. Al-Hashimi, J.H. Prestegard, Rapid determination of protein folds using residual dipolar couplings, J. Mol. Biol. 304 (2000) 447–460.
[28] G.M. Clore, M.R. Starich, M. Bewley, M. Cai, J. Kuszewski, Impact of residual dipolar couplings on the accuracy of NMR structures determined from a minimal number of NOE restraints, J. Am. Chem. Soc. 121 (1999) 6513–6514.
[29] A.W. Giesen, S.W. Homans, J.M. Brown, Determination of protein global folds using backbone residual dipolar coupling and long-range NOE restraints, J. Biomol. NMR 25 (2003) 63–71.
[30] A.M.J.J. Bonvin, K. Houben, M. Guenneugues, R. Kaptein, R. Boelens, Rapid fold determination using secondary chemical shifts and cross-hydrogen bond ^{15}N–$^{13}C'$ scalar couplings (3hbJNC'), J. Biomol. NMR 21 (2001) 221–233.
[31] L.M.I. Koharudin, A.M.J.J. Bonvin, R. Kaptein, R. Boelens, Use of very long-distance NOEs in a fully deuterated protein: an approach for rapid protein fold determination, J. Magn. Reson. 163 (2003) 228–235.
[32] A.A. Bothner-By, C. Gayathri, P.C.M. Van Zijl, C. Maclean, J.-J. Lai, K.M. Smith, High-field orientation effects in the high-resolution proton NMR spectra of diverse porphyrins, Magn. Reson. Chem. 23 (1985) 935–938.
[33] F. Arnesano, L. Banci, I. Bertini, J. Faraone-Mennella, A. Rosato, P.D. Barker, A.R. Fersht, The solution structure of oxidized *Escherichia coli* cytochrome b_{562}, Biochemistry 38 (1999) 8657–8670.
[34] F. Arnesano, L. Banci, I. Bertini, K. van der Wetering, M. Czisch, R. Kaptein, The auto-orientation in high magnetic field of oxidized cytochrome b_{562} as source of constraints for solution structure determination, J. Biomol. NMR 17 (2000) 295–304.
[35] N. Tjandra, A. Bax, Measurement of dipolar contributions to $^1J_{CH}$ splittings from magnetic-field dependence of J modulation in two-dimensional NMR spectra, J. Magn. Reson. 124 (1997) 512–515.
[36] D.S. Wishart, B.D. Sykes, The ^{13}C chemical shift index: a simple method for the identification of protein secondary structure using ^{13}C chemical shift data, J. Biomol. NMR 4 (1994) 171–180.
[37] L. Banci, I. Bertini, K.L. Bren, M.A. Cremonini, H.B. Gray, C. Luchinat, P. Turano, The use of pseudocontact shifts to refine solution structures of paramagnetic metalloproteins: Met80Ala cyano-cytochrome *c* as an example, J. Biol. Inorg. Chem. 1 (1996) 117–126.
[38] L. Banci, I. Bertini, G. Gori Savellini, A. Romagnoli, P. Turano, M.A. Cremonini, C. Luchinat, H.B. Gray, The pseudocontact shifts as constraints for energy minimization and molecular dynamic calculations on solution structures of paramagnetic metalloproteins, Proteins Struct. Funct. Genet. 29 (1997) 68–76.
[39] J.H. Prestegard, H.M. Al-Hashimi, J.R. Tolman, NMR structures of biomolecules using field oriented media and residual dipolar couplings, Q. Rev. Biophys. 33 (2000) 371–424.
[40] I. Bertini, C. Luchinat, G. Parigi, Paramagnetic constraints: an aid for quick solution structure determination of paramagnetic metalloproteins, Concepts Magn. Reson. 14 (2002) 259–286.
[41] M. Allegrozzi, I. Bertini, M.B.L. Janik, Y.-M. Lee, G. Liu, C. Luchinat, Lanthanide induced pseudocontact shifts for solution structure refinements of macromolecules in shells up to 40 Åfrom the metal ion, J. Am. Chem. Soc. 122 (2000) 4154–4161.
[42] I. Bertini, Y.-M. Lee, C. Luchinat, M. Piccioli, L. Poggi, Locating the metal ion in calcium-binding proteins by using cerium(III) as a probe, ChemBioChem. 2 (2001) 550–558.
[43] R. Barbieri, I. Bertini, G. Cavallaro, Y.-M. Lee, C. Luchinat, A. Rosato, Paramagnetically induced residual dipolar couplings for solution structure determination of lanthanide-binding proteins, J. Am. Chem. Soc. 124 (2002) 5581–5587.
[44] J. Feeney, B. Birdsall, A.F. Bradbury, R.R. Biekofsky, P.M. Bayley, Calmodulin tagging provides a general method of using lanthanide induced magnetic field orientation to observe residual dipolar couplings in proteins in solution, J. Biomol. NMR 21 (2001) 41–48.
[45] J. Wöhnert, K.J. Franz, M. Nitz, B. Imperiali, H. Schwalbe, Protein alignment by a coexpressed lanthanide-binding tag for the measurement of residual dipolar couplings, J. Am. Chem. Soc. 125 (2003) 13338–13339.
[46] M. Gochin, H. Roder, Protein structure refinement based on paramagnetic NMR shifts. Applications to wild-type and mutants forms of cytochrome *c*, Protein Sci. 4 (1995) 296–305.
[47] I. Bertini, A. Donaire, C. Luchinat, A. Rosato, Paramagnetic relaxation as a tool for solution structure determination: *Clostridium pasterianum* ferredoxin as an example, Proteins Struct. Funct. Genet. 29 (1997) 348–358.
[48] I. Bertini, M.M.J. Couture, A. Donaire, L.D. Eltis, I.C. Felli, C. Luchinat, M. Piccioli, A. Rosato, The solution structure refinement of the paramagnetic reduced HiPIP I from *Ectothiorhodospira halophila* by using stable isotope labeling and nuclear relaxation, Eur. J. Biochem. 241 (1996) 440–452.
[49] F. Arnesano, L. Banci, I. Bertini, I.C. Felli, C. Luchinat, A.R. Thompsett, A strategy for the NMR characterization of type II copper(II) proteins: the case of the copper trafficking protein CopC from *Pseudomonas syringae*, J. Am. Chem. Soc. 125 (2003) 7200–7208.

[50] I. Bertini, G. Cavallaro, M. Cosenza, R. Kummerle, C. Luchinat, M. Piccioli, L. Poggi, Cross correlation rates between curie spin and dipole–dipole relaxation in paramagnetic proteins: the case of cerium substituted calbindin D_{9k}, J. Biomol. NMR 23 (2002) 115–125.
[51] P. Turano, G. Battaini, L. Casella, Validation of paramagnetic cross correlation rates for solution structure determination of high spin iron(III) heme proteins, Chem. Phys. Lett. 373 (2003) 460–463.
[52] P.B. Barker, E.P. Nerou, S.M.V. Freund, I.M. Fearnley, Conversion of cytochrome b_{562} to c-type cytochromes, Biochemistry 34 (1995) 15191–15203.
[53] S. Grzesiek, A. Bax, Correlating backbone amide and side chain resonances in larger proteins by multiple relayed triple resonance NMR, J. Am. Chem. Soc. 114 (1992) 6291–6293.
[54] S. Grzesiek, A. Bax, An efficient experiment for sequential backbone assignment of medium-sized isotopically enriched proteins, J. Magn. Reson. 99 (1992) 201–207.
[55] A. Bax, G.M. Clore, P.C. Driscoll, A.M. Gronenborn, M. Ikura, L.E. Kay, Practical aspects of proton-carbon–carbon-proton three dimensional correlation spectroscopy of ^{13}C-labeled proteins, J. Magn. Reson. 87 (1990) 620–627.
[56] L. Emsley, G. Bodenhausen, Optimization of shaped selective pulses for NMR using a quaternion description of their overall propagators, J. Magn. Reson. 97 (1992) 135–148.
[57] C. Bartels, T.H. Xia, M. Billeter, P. Güntert, K. Wüthrich, The program XEASY for computer-supported NMR, J. Biomol. NMR 5 (1995) 1–10.
[58] L. Werbelow, Dynamic frequency shift, in: D.M. Grant, R.K. Harris (Eds.), Encyclopedia of Nuclear Magnetic Resonance, Wiley, Chichester, 1996.
[59] E.C.I. Veerman, Carbon-13 chemical shift anisotropy, Progr. NMR Spectrosc. 16 (1984) 193–235.
[60] L. Banci, I. Bertini, M.A. Cremonini, G. Gori Savellini, C. Luchinat, K. Wüthrich, P. Güntert, PSEUDODYANA for NMR structure calculation of paramagnetic metalloproteins using torsion angle molecular dynamics, J. Biomol. NMR 12 (1998) 553–557.
[61] R. Koradi, M. Billeter, K. Wüthrich, MOLMOL: a program for display and analysis of macromolecular structure, J. Mol. Graph. 14 (1996) 51–55.
[62] P. Guentert, C. Mumenthaler, K. Wüthrich, Torsion angle dynamics for NMR structure calculation with the new program DYANA, J. Mol. Biol 273 (1997) 283–298.
[63] The target function is proportional to the quadratic sum of deviation between experimental and calculated constraints. It provides a measure of how well the structure satisfies experimental constraints used for structure calculations. For the exact definition see references [5,60,62].
[64] A.T. Bruenger, G.M. Clore, A.M. Gronenborn, R. Saffrich, M. Nilges, Assessing the quality of solution structures by complete cross-validation, Science 261 (1993) 328–331.
[65] G.M. Clore, D.S. Garrett, R-factor, Free R and complete cross-validation for dipolar coupling refinement of NMR structures, J. Am. Chem. Soc. 121 (1999) 9008–9012.